ELSEVIER

Journal of Power Sources 114 (2003) 96–104

JOURNAL OF POWER SOURCES

www.elsevier.com/locate/jpowsour

Investigation on solvent-free solid polymer electrolytes for advanced lithium batteries and their performance

Y. Aihara*, J. Kuratomi, T. Bando, T. Iguchi, H. Yoshida, T. Ono, K. Kuwana

Yuasa Corporation, 4-5-1 Ohgi-Cho, Odawara-Shi 250-0001, Kanagawa, Japan

Received 4 March 2002; received in revised form 29 August 2002; accepted 26 September 2002

Abstract

Seven solvent-free solid polymer electrolytes based on cross-linked polyethers and doped with $LiN(CF_3SO_2)_2$, were investigated for usage in large-scale rechargeable lithium batteries. They are classified into two categories: one contains five poly(ethyleneoxide-co-propyleneoxide) (poly(EO-co-PO)) network polymers with different degrees of cross-linking and precursor molecular weight and the other includes two polyethers with borate structure having a Lewis acid functionality as an anion trap. The ionic conductivity, direct current characteristics, thermal properties and transference numbers were measured. To evaluate the battery performance for the polymer electrolytes, test cells of the typical Li/solvent-free solid polymer electrolyte/$LiCoO_2$, were fabricated. High discharge performance was obtained for the solvent-free electrolytes made of the less cross-linked poly(EO-co-PO) and for the PEO including borate structure. A 10 Wh class lithium battery was entirely fabricated from solid components, and 500 charge–discharge cycles with 100% capacity retention was demonstrated. The present limitations and problems for further improvement of polymer batteries are also discussed.

Keywords: Solvent-free polymer electrolyte; Cell performance; Lithium battery; Transference number; Ionic conductivity

1. Introduction

Solid polymer electrolytes have been paid much attention in the last two decades to use in various electrochemical devices. Since the discovery of solid polymer electrolytes, many efforts have been made to improve the electrochemical and thermal properties. Solvent-free solid polymer electrolytes used in rechargeable lithium batteries are mainly based on cross-linked poly(ethyleneoxide-co-propyleneoxide) (poly(EO-co-PO)) [1] with doping lithium bis(trifluoromethansulfonyl)imide (LiTFSI) and are amorphous at room temperature [2]. They are prepared by polymerization of monomers containing acryloyl groups ($OCOCH{=}CH_2$) in place of the terminal OH [3]. Kono et al. modified the precursor monomer by partially replacing the terminal OH groups with methyl groups CH_3 before the acrylation reaction to increase the degree of free chain structure in the cross-linked frame, and succeeded in increasing the ionic conductivity [4]. Similar trials, such as cross-linking of the polyether [5] and introducing a comb structure [6], also increased the ionic conductivity and decreased the glass transition temperature. The introduction of a functional group into the polymer structure resulted in high lithium transference numbers in polyethers based on a boroxine host [7,8]. The application of the polyethyleneglycol (PEG) borate polymer electrolyte for lithium battery has been also reported [9].

Our strategy in developing solvent-free lithium polymer batteries was the following. First, improving conventional polymers electrolytes and adopting new polymer electrolytes. In this stage we chose five different poly(EO-co-PO) with different degrees of cross-linking by introducing partial methylation in the precursor and various polymer sizes. In addition, two new novel borate polymers were synthesized in order to increase the transference number of lithium ion. The polymer electrolytes were evaluated by measuring the ionic conductivity, limiting current density, transference number and thermal properties.

The second stage involved making test cells including suitable cathodes and anodes. The test cells were fabricated using the seven polymer electrolytes and the capacity retention and rate capability were determined. Further, a 10 Wh

* Corresponding author. Tel.: +81-465-2245; fax: +81-465-2241.
E-mail address: yuichi.aihara@nifty.ne.jp (Y. Aihara).

0378-7753/02/$ – see front matter © 2002 Elsevier Science B.V. All rights reserved.
PII: S0378-7753(02)00529-3

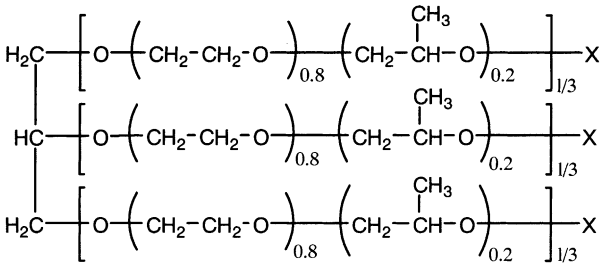

poly(EO-*co*-PO)s

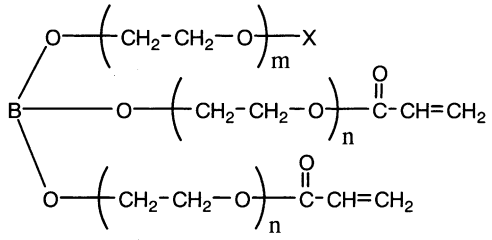

PEOBs

Fig. 1. Chemical structure of the precursors: poly(EO-co-PO)- and poly(ethyleneoxide)-based borates (X = methyl or acryloyl group in the figure).

class battery was fabricated and demonstrated to have long charge–discharge processes by using one of the seven candidate polymer electrolytes as the electrolyte and another as a separator.

In the third stage, the fundamental relationships between ionic conduction and diffusion phenomena were investigated to enable the development of practical large-scale batteries. We have reported the correlation of ion self-diffusion coefficients with ionic conduction [10–13].

Here we report the present status of the solvent-free polymer lithium batteries that we have developed and discuss the problems to be solved for the development of practical and commercial lithium polymer batteries.

2. Experimental procedure

2.1. Preparation of solvent-free polymer electrolytes

The poly(EO-co-PO) precursors were obtained from Daiichi Kogyo Seiyaku (Kyoto). The structures of the precursor macromonomers are shown in Fig. 1 and their properties are listed in Table 1. To control the cross-linking degree, the methylation of the terminal OH in the EO-co-PO was made in a random way and the remaining OH groups were acrylated.

The two precursor PEO-based borates were synthesized by dehydration condensation of polyethyleneglycol by using B_2O_3, and the OH were replaced by acryloyl groups before the cross-linking reaction and dried. The residual water contents were measured by the Carl Fisher method and were less than 50 and 200 ppm for EO-co-PO and PEOB, respectively. The seven precursors were all viscous liquids, and LiTFSI was directly dissolved by using a magnetic stirrer at 60 °C for 48 h. The salt concentration was fixed at O/Li = 10/1 (where O represents is the ether oxygen) for all polymer electrolytes. The solution was cast on a stainless steel plate and irradiated by using an electron beam (10 Mrad) under a nitrogen atmosphere. The thickness of the membrane was approximately 150 μm.

Table 1
Seven solvent-free polymer electrolytes

Sample	Precursor molecular weight	Termination	Host unit
80PE00	8000	All acrylated	EO-co-PO[a]
80PE20	8000	20 mol% methylated[b]	EO-co-PO
80PE50	8000	50 mol% methylated	EO-co-PO
32PE50	3200	50 mol% methylated	EO-co-PO
11PE50	1100	50 mol% methylated	EO-co-PO
PEOB-TA	1200	All acrylated	EO borate[c]
PEOB-DA	1400	Partially methylated[d]	EO borate[e]

[a] The main chain was composed of random co-polymer of ethyleneoxide and propyleneoxide.
[b] Twenty mole percent of the terminal OH were methylated before acrylation.
[c] The main chain was composed of ethyleneoxide units. The three chains consisted of about nine units of EO each.
[d] One of three terminal OH was terminated by methyl group. The remaining two were terminated by acryloyl groups.
[e] The methyl terminated chain was consisted of about 23 units of EO (long chains).

2.2. Electrochemical and DSC measurements

The ionic conductivity, limiting current density, potential stability and transference number were determined for the polymer electrolyte membranes. The ionic conductivity was determined using the ac impedance method on a Solartron Electrochemical Interface 1286 and Frequency Response Analyzer 1255. The solvent-free polymer electrolyte samples (13 mm in diameter and approximately 100 μm thick) were put into two identical nickel blocking electrodes. The electrodes were packed in a sealed cell with a nickel current corrector. The impedance measurements were carried out from 0.1 Hz to 1 MHz in the temperature range 30–80 °C. The ionic conductivity was calculated from the bulk resistance and cell constant. Also non-blocking electrodes of metal lithium were used for determining charge-transfer resistance (R_{CT}). R_{CT} was determined from a semi-circle of the impedance spectra, which was a component of the electron charge-transfer resistance according to the literature [14].

The linear sweep chronopotentiometry and cyclic voltammetry (CV) were performed on an automatic polarization system HZ3000 (Hokuto Denko). Electrochemical cells consisting of 20 mm × 20 mm of metal lithium (thickness was 100 μm) working electrode with nickel current corrector, 50 mm × 50 mm polymer electrolyte membrane (thickness was approximately 100 μm) and 40 mm × 40 mm of

metal lithium (thickness was 100 μm) counter electrode with nickel current corrector were fabricated. A Li/Li^+ reference (with nickel lead) was used. The cells were stacked and vacuum sealed in a laminated aluminum bag. The electrochemical cells for measuring CV were similar to the above, however, for observing cathodic and anodic decomposition, nickel and aluminum working electrodes were used, respectively. In the linear sweep chronopotentiometry, the current sweep rate was 2 μA s^{-1} and the measurement was finished when the voltage achieved 5 V. In the CV measurement, a voltage sweep rate of 10 mV s^{-1} was used. The sweep voltage range was 0.5–4.5 V for confirming the anodic decomposition and 0–3 V for the cathodic decomposition. All measurements were performed at 60 °C.

The lithium ion transference number (t^+) was determined using the dc polarization/ac impedance combination method [15]. A constant potential of 10 mV was applied the electrodes for the polarization. Hence, t^+ is given by

$$t^+ = \frac{I_s(\Delta V - I_0 R_0)}{I_0(\Delta V - I_s R_s)} \quad (1)$$

where the I_0 and I_s are the current at the initial and steady states, respectively. R_0 and R_s are the passivating layer resistances at the initial and steady states, respectively. The measurements were performed at 60 °C.

Differential scanning calorimetry (DSC) measurements were performed using a DSC220C differential scanning calorimeter (Seiko Electronics). The samples were sealed in aluminum pans and scanned from −150 to 80 °C with a scanning rate of 10 °C min^{-1}. The glass transition temperature (T_g) was determined from the midpoint of the heat capacity changes.

2.3. Fabrication and characterization of test cells and 10 Wh class batteries

Test cells and a 10 Wh class battery fabricated with a typical metal Li (anode)–$LiCoO_2$ (cathode) configuration with a solvent-free polymer electrolyte. Poly(vinyliden fluoride) (PVdF) was used as a binder. The cathode electrode was constructed on an aluminum foil by printing composite (ground $LiCoO_2$ and acetylene black were dispersed/dissolved in *N*-methyl pyrolidone), and after removal of the solvent, the cathode cavity was first filled the liquid precursor macromonomer doped with LiTFSI (the salt concentration was O/Li = 10/1). Then doped precursor macromonomer was carefully added to the cathode to a thickness of about 30 μm and then irradiated with an electron beam (10 Mrad) to produce the solvent-free polymer electrolyte–separator layer inside the cathode electrode.

To determine a suitable thickness of the polymer electrolytes, several cathode electrodes were prepared by using completely cross-linked poly(EO-co-PO) (80PE00) for testing the rate capability.

A 10 Wh class solvent-free polymer lithium battery was constructed by winding aluminum foil (current corrector)/cathode/polymer electrolyte/Li metal/copper foil. The cycle ability for the test cells and 10 Wh class polymer batteries was obtained by the constant current/constant voltage (CC/CV) charge–constant current (CC) discharge at *C*/8 at 60 °C. The operating voltage was in the range of 3.0–4.1 V. The fabricated cells are summarized in Table 2.

Table 2
Test cells and 10 Wh class battery configuration

Cell	Electrolyte in cathode	Separator layer	Cathode thickness (μm)	Capacity (mAh, as prepared)
A	80PE00	80PE00	30 (50, 60)	10 (17, 20)
B	80PE20	80PE20	30	10
C	80PE50	80PE50	30	10
D	32PE50	80PE00[a]	30	10
E	11PE50	80PE00[a]	30	10
F	PEOB-TA	PEOB-TA	30	10
G	PEOB-DA	PEOB-DA	30	10
H	32PE50	80PE00	30	2740

[a] 32PE50 and 11PE50 could not be applied to the separator layer due to their fragility.

3. Results

3.1. Thermal characteristics

The DSC curves for all the solvent-free polymer electrolytes are given in Fig. 2. No melting/crystalline peaks were observed for any of the electrolytes, and the glass transition (T_g) was observed in the curves between 240 and 246 K, except for 11PE50 and PEOB-TA. Although those two

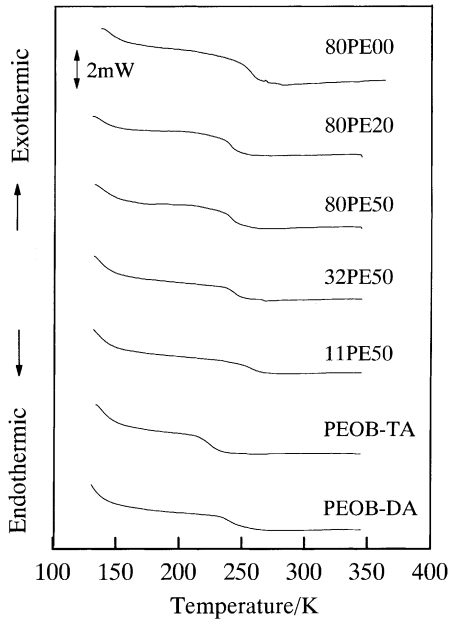

Fig. 2. DSC traces of the seven polymer electrolytes. The figure shows DSC traces during heating scan from −150 to 80 °C. The scanning rate was 10 °C min^{-1}.

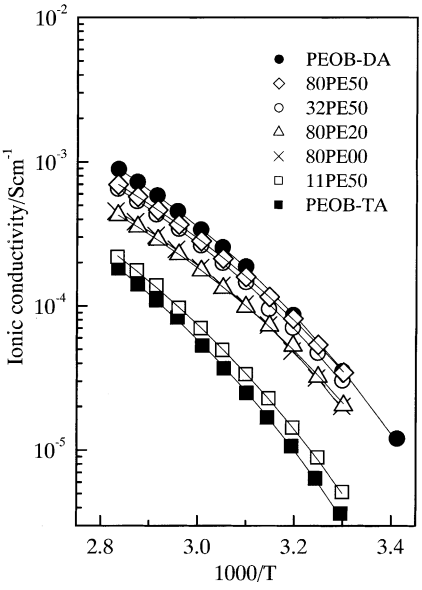

Fig. 3. Arrhenius plots of the ionic conductivity for the seven polymer electrolytes. The solid lines are the result of regressing the VTF equation onto the data.

polymers were structurally rigid due to low molecular weight of macromonomer (the cross-linking distance depends on the molecular size of monomers), PEOB-TA showed the lowest T_g, and 11PE50 had the highest T_g among all the polymer electrolytes. Generally, T_g increases with increasing cross-linking density, however, a low T_g (225 K) was observed for PEOB-TA. The absence of crystalline phases suggests that all of the polymer electrolytes are amorphous over the whole temperature range.

3.2. Ionic conductivity of the solvent-free polymer electrolytes

Arrhenius plots of the ionic conductivity for the seven polymer electrolytes are given in Fig. 3. The temperature dependence of the ionic conductivity showed convex curvature and was well described by the Vogel–Tamman–Fulcher (VTF) equation (2). The results of regressing

Table 3
VTF parameters for the seven polymer electrolytes

Sample	VTF parameters			DSC T_g (K)
	A (S cm^{-1} K$^{-1/2}$)	B (K)	T_0 (K)	
80PE00	1.69	682	222	246
80PE20	4.62	872	208	240
80PE50	4.57	850	209	242
32PE50	2.46	704	220	243
11PE50	3.98	947	215	257
PEOB-TA	3.85	948	218	225
PEOB-DA	5.65	801	215	244

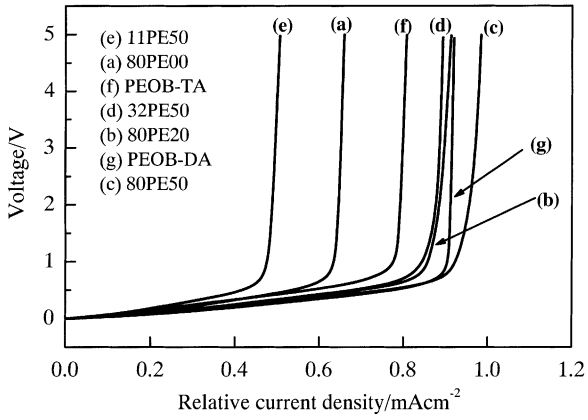

Fig. 4. Current–potential profile (I–V) curves of the seven polymer electrolytes. The current density is a relative value.

Eq. (2) onto the data are summarized in Table 3.

$$\sigma(T) = AT^{-1/2}\exp\left(-\frac{B}{T-T_0}\right) \quad (2)$$

Two polymer electrolytes, PEOB-TA and 11PE50, gave lower ionic conductivity in comparison with the other polymer electrolytes. The order of the ionic conductivity at 353 K was PEOB-DA > 80PE50 > 32PE50 > 80PE20 ≅ 80PE00 ⩾ 11PE50 > PEOB-TA. In the poly(EO-co-PO), the highest ionic conduction was observed for 80PE50. Comparing 80PE50, 32PE50 and 11PE50, which have the same degree of cross-linking, reveals that the ionic conductivity is influenced by the precursor molecular size. The higher ionic conductivity of PEOB-DA compared to PEOB-TA results from enhancement of side chain mobility in the polymer structure.

3.3. Limiting current of the polymer electrolytes

The current–potential profile (I–V) curves of the solvent-free polymer electrolytes at 60 °C are shown in Fig. 4. Usually, the limiting current density depends on the voltage or current scanning rate. The current scanning rate of 2 μA s^{-1} was used, the observed limiting current are relatively available to compare as the present values in these experiments. The voltage profile changed with increasing the current density according to Ohm's law and the cell potential increased significantly when the polarization occurred. The order of relative limiting current, I^R_{lim} was PEOB-DA ≅ 80PE50 > 32PE50 > 80PE20 > PEOB-TA > 80PE00 > 11PE50. The order is similar to that of the ionic conductivity at 60 °C, except for PEOB-TA.

3.4. Lithium transference number, t^+

The t^+, determined by the dc polarization–ac impedance combination method (i.e. Evance et al.'s method [15]) are summarized in Table 4. As we reported previously, t^+ in 80PE00 was 0.05 [2], and similar values were obtained in

Table 4
The transference number of Li^+ for the seven polymer electrolytes at 333 K

Sample	R_0 (Ω)	R_s (Ω)	I_0 (A)	I_s (A)	Transference number (t^+)
80PE00	17.41	18.76	9.05×10^{-5}	8.19×10^{-6}	0.05
80PE20	17.00	18.35	1.09×10^{-4}	6.93×10^{-6}	0.05
80PE50	14.50	14.97	1.28×10^{-4}	8.25×10^{-6}	0.05
32PE50	36.71	31.70	7.54×10^{-5}	4.61×10^{-6}	0.05
11PE50	50.38	58.86	2.95×10^{-5}	1.60×10^{-6}	0.05
PEOB-TA	36.37	42.10	3.35×10^{-5}	4.80×10^{-6}	0.13
PEOB-DA	8.95	5.84	1.25×10^{-4}	2.05×10^{-5}	0.15

other poly(EO-co-PO) electrolytes. The PEO-based polymer electrolytes doped with LiTFSI generally have low transference numbers [3], and thus the present results are reasonable. The low t^+ indicates that the ionic conductivity mainly depends on anion transport. Also t^+ does not depend on the polymer cross-linking density. Higher t^+ values were obtained in the two electrolytes having borate structure. The t^+ of PEOB-DA was 0.15, and three times larger than that of EO-co-PO electrolytes.

3.5. Discharge rate and cycle characteristics of the test cells

The cycle ability of the test cells at 60 °C are given in Fig. 5 where the cell capacities showed a clear dependence on the polymer electrolytes. Since reversible capacities of $LiCoO_2$ are known to be between 120 and 135 mAh g^{-1} [16], cells B and C almost reached the limiting capacity. Stable capacities were achieved in cells A, D and G with 110–90 mAh g^{-1} and less than 50 mAh g^{-1} in cells E and F. Cells E and F, which were made of rigid polymer electrolytes 11PE50 (cell E) and PEOB-TA (cell F), had the lowest capacity performance.

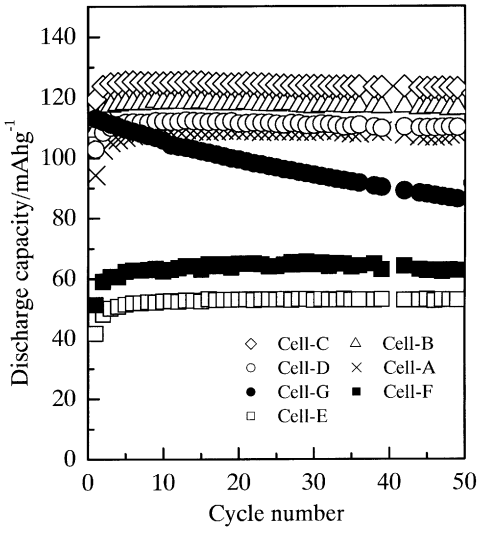

Fig. 5. Cycle characteristics of test cells using various polymer electrolytes.

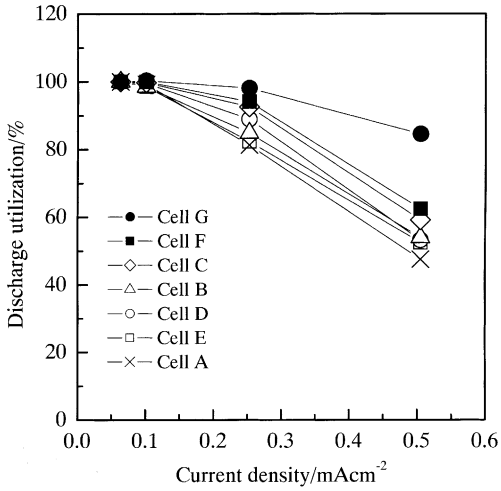

Fig. 6. Discharge rate characteristics of test cells using various polymer electrolytes. The data were normalized to a discharge capacity at 0.06 mA cm^{-2}.

Except for cell G, good cycle performances were achieved with full capacity retention until 50 cycles.

The discharge utilization was estimated as follows. The initial capacity at *C*/8 was set as 100% for each cell, and the utilization at the discharge current was divided by the capacity at *C*/8 as shown in Fig. 6. Almost all the cells achieved approximately 100% utilization until 0.1 mA cm^{-2} (*C*/5) discharge, however, the discharge utilization decreased significantly at 1*C*, except for cell G. The discharge rate at 0.1 mA cm^{-2} (*C*/5) was the limiting current density for most of the test cells. The order of the rate capability at 0.5 mA cm^{-2} (1*C*) were cells G ≫ F ≅ C > B ≅ D ≅ E > A.

Remarkably, cell G showed the best performance in spite of the faster decrease of the discharge capacity by cycle number as shown in Fig. 5. The rate capability of cell F was much higher than that of cell E even though the each cells used similar low ionic conduction polymer electrolytes.

Of the present samples, the best performance was obtained in for cell C, although the rate capability was lower than that of cell G.

3.6. Correlation between cathode thickness and rate capability

The relationship between discharge capacity and current density is shown for various thickness of the cathode in Fig. 7. The charge rate was first fixed at 0.125*C* (the discharge was actually performed by the *C*-rate, the discharge current at 0.125*C* is the lowest current density in Fig. 7) for each cell, and the discharge rate was varied. It was clearly shown that the discharge capacity decreases with increasing discharge current density. Discharge capacities of 105, 78 and 60 mA g^{-1} at the observable lowest discharge current density were measured for the 30, 50 and 60 μm cathodes, respectively. We also confirmed the maximum discharge capacity at very low current, 0.01*C* and found the

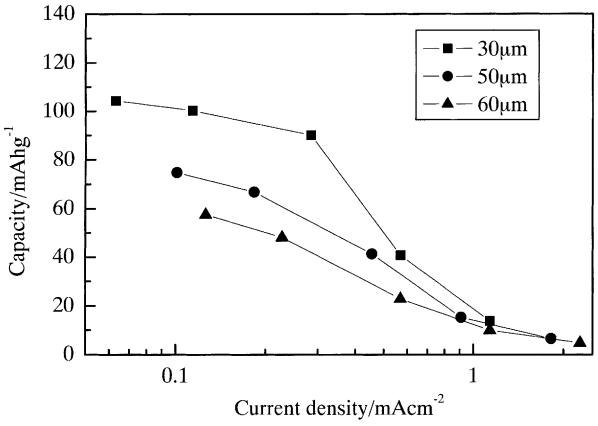

Fig. 7. Discharge rate characteristics of the test cells which are composed of various thicknesses of cathode. LiTFSI-doped 80PE00 was used for the polymer electrolyte.

discharge capacities were 115.3, 115.4 and 117.8 mAh g^{-1} with cathode thicknesses of 30, 50 and 60 μm, respectively.

3.7. Demonstration of 10 Wh class battery

A 10 Wh class battery was fabricated by using the 32PE50 and 80PE50 as the electrolyte and separator in cathode, respectively, and the discharge capacity versus the cycles achieved at 60 °C is shown in Fig. 8. The capacity retention was maintained until at least 500 cycles. The charge–discharge curves of the battery are shown in Fig. 9. Although no capacity retention was observed in Fig. 8, increasing resistive components must be considered because of the differences in the discharge curves between the first and 355 cycles in Fig. 9. Since the main purpose of the test battery was to establish the solvent-free lithium battery having reasonable cycle performance, high energy density was not an important target. The energy densities per weight and volume were 62.8 Wh kg^{-1} and 124.5 Wh l^{-1}, respectively, where electrodes including current collectors and solid polymer electrolyte were taken into account but the battery case was excluded.

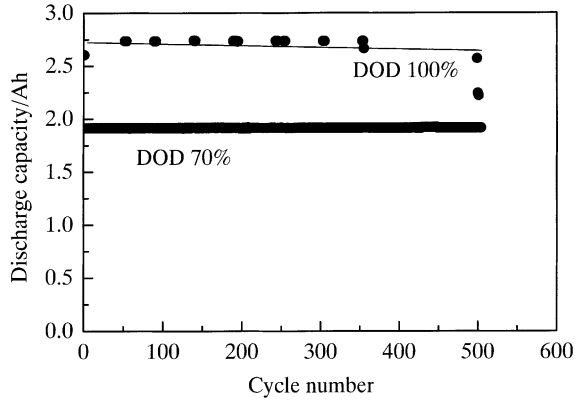

Fig. 8. Cycle characteristic of a 10 Wh class battery. The battery charged by *C*/7 (CC/CV) and discharged by *C*/8 (CC). The cut off voltages were 4.1 V for the upper and 3.0 V for the lower limit (DOD = 100%). For DOD = 70%, the discharge capacity was controlled by a specified time (5.6 h).

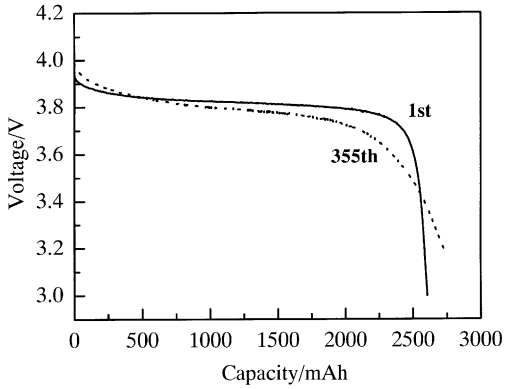

Fig. 9. Discharge curves for the 1st (solid line) and 355th (dotted line) cycle of the 10 Wh class battery.

4. Discussion

4.1. Correlation of electrochemical and thermal properties for the seven polymer electrolytes

The ionic conductivity is the most important parameter for evaluating the solid polymer electrolytes and is closely related to the limiting current density in the charge–discharge process, which gives the available charge–discharge capacity in batteries at high current. Comparison between the limiting currents in Fig. 4 and the ionic conductivities in Fig. 3 indicates that the order in the magnitude in the ionic conductivity is similar to that of the limiting current density except for the rigid electrolytes, PEO-TA and 11PE50. These two electrolytes have lower ionic conductivity and similar temperature dependence because of the lower polymer chain mobility of shorter cross-linked chains. However, the relative limiting current density of PEOB-TA was higher than that of 11PE50, and it could be interpreted that the larger t^+ in PEOB-TA induced the larger relative limiting current density. This result clearly shows that the high t^+ (i.e. high cation conductivity) is needed for high performance of polymer electrolytes. On the other hand, in 80PE50 and PEOB-DA, which have larger limiting current densities, the t^+ of the latter is three times larger than the former. But the ionic conductivity, apparent limiting current and glass transition temperatures are almost the same for both electrolytes. To understand the details, more molecular level studies are necessary.

The ionic conductivity increased with decreasing the cross-linking density (i.e. 80PE00 < 80PE20 < 80PE50) for same precursor size. The limiting current density increased in the order 80PE00 ⋘ 80PE20 < 80PE50. It is also important to consider the charge-transfer resistance between the polymer electrolyte and lithium metal in anode.

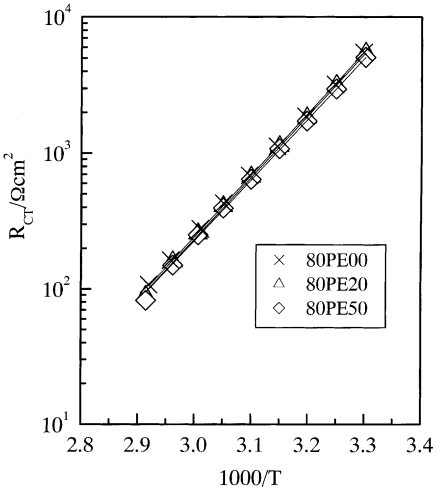

Fig. 10. An Arrhenius plot of the charge-transfer resistances (R_{CT}) for 80PE00, 80PE20 and 80PE50. The solid lines are the result of the single exponential regressed onto the data.

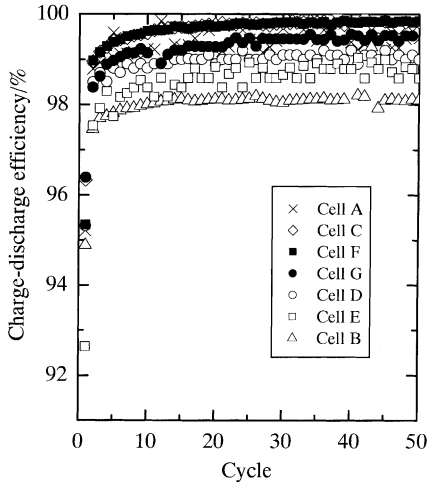

Fig. 11. The charge–discharge efficiency of the test cells using various polymer electrolytes.

Arrhenius plots of the resistance, which corresponds to interface of polymer electrolyte and lithium anode, i.e. charge-transfer resistance (R_{CT}), is shown in Fig. 10. The temperature dependence of R_{CT} for the 80PE series was very close. This indicates that the activation energy of R_{CT} for those electrolytes are also close, thus the difference of the relative limiting current density for those electrolytes may not be depended on the R_{CT}. Generally, the electrolytes having higher ionic conductivity gave the higher limiting current density in the present solvent-free polymer electrolytes. At least, the limiting current is not affected by the R_{CT} for 80PE series. At the present salt concentration, the ions enter in pseudo-cross-linking positions to form macroscopic homogeneous structures and affect the interface behavior.

4.2. Correlation between cell performance and polymer electrolyte properties

The test cell performances were clearly influenced by electronic properties, especially the ionic conductivity of the polymer electrolytes. For example, the discharge capacity of 11PE50 and PEOB-TA cells were 50–60 mAh g^{-1} and was a half or one-third of the capacity of other polymer electrolyte cells and their ionic conductivities were also around one third of other polymer electrolytes.

During the first few cycles, the discharge capacity increased in all the cells as shown in Fig. 11 where the charge–discharge efficiency (Q_{eff}) is plotted versus the cycle number. The cells showed stable capacity retention after approaching the equilibrium state, this implies that side reactions or decomposition occurred in the initial few cycles.

To clarify the cause of low Coulombic efficiency, especially in the first cycle, the electrochemical stability was measured by cyclic voltammetry. Fig. 12 shows the cyclic voltammograms for all the polymer electrolytes. Fig. 12(a) shows the anodic decomposition using an aluminum working electrode. In the first cycle of each trace, anodic current was observed in the range of 3–4 V and decreased and became smaller according to the increasing cycles. The anodic current at the first cycle may be related to the decomposition of a part of the polymer electrolytes at cathode interfaces. As the cathodic decomposition in each polymers (see Fig. 12(b)), large cathodic current was detected in the first cycle for all the polymers and the current decreased significantly in the third cycle. The reduction and oxidation appear to be irreversible reactions. In the third cycle, a small current was still observed in PEOB-DA. It is not known why the PEO-DA decomposes at lower voltages, although the PEOB-TA which has a similar chemical structure, is electrochemically stable, and the remaining OH in PEO-DA might be the origin of the decomposition. The anodic and cathodic decomposition may give rise to a solid electrolyte interface (SEI) [17], which must contribute to the low Coulombic efficiency in the first few cycles. The improvement of the interface between active materials and polymer electrolytes is necessary especially for rocking chair type batteries because high Coulombic efficiency is required.

Although the fabricated 10 Wh class battery achieved more than 500 charge–discharge cycles, the voltage profile at discharge decreased after 300 cycles. One cause might originate in the capacity of the lithium (anode). We designed a 10 times larger capacity for lithium anode compared to cathode capacity and applied it to the test batteries. The expected figure of merit (FOM) must be larger than 50 after 500 and longer cycles at 100% deep of discharge (DOD). It is known that the FOM is lower than 50 in liquid electrolytes for lithium batteries [18,19]. At present, our test battery achieved 500 cycles at 70% DOD, which means that the FOM may be less than 50. In order to obtain longer cycles by using solid electrolytes, efforts to increase FOM are still required. The 10 Wh class battery showed good perfor-

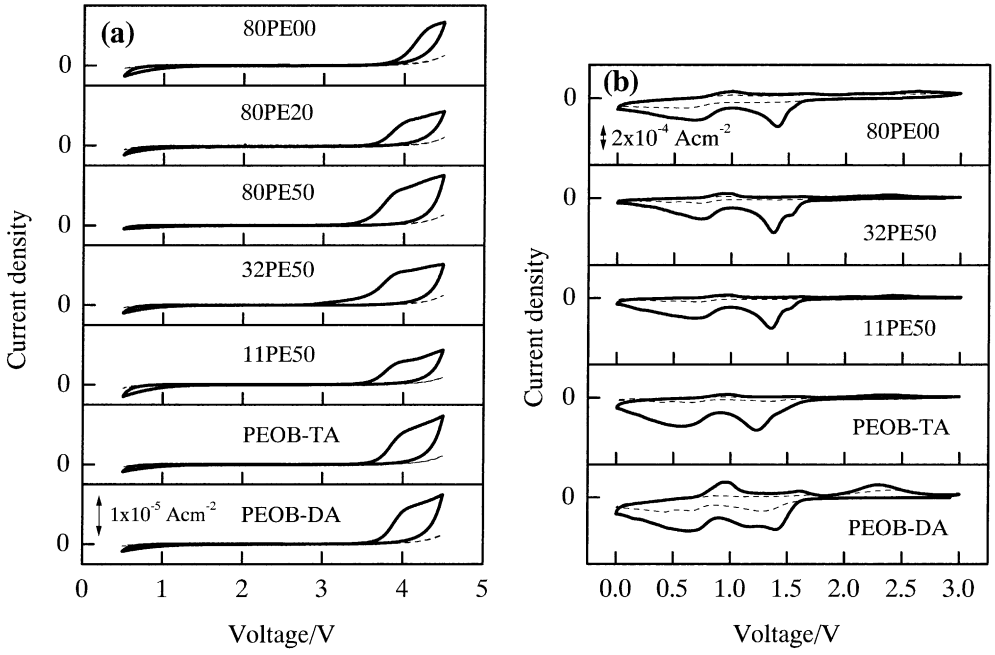

Fig. 12. Cyclic voltammograms of the various polymer electrolytes: (a) anodic decomposition; (b) cathodic decomposition.

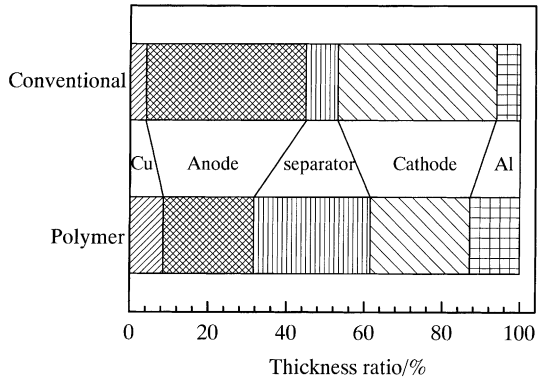

Fig. 13. Battery design and the thickness ratio, which corresponds to cell components for polymer and conventional (liquid) type lithium ion batteries.

mance during 500 cycles at 70% DOD, which indicates the possibility of longer cycle ability using lithium metal. From our trials, we found the thickness of the components is important to fabricate large-scale batteries and the best composition thickness ratio of the electrochemical components in the present stage is shown in Fig. 13. The lithium ion conduction estimated from the lithium ion self-diffusion coefficients in these polymer electrolytes is not good enough compared with the solution electrolyte batteries, for example, the lithium self-diffusion coefficient in 80PE00 is 8.0×10^{-12} m^2 s^{-1} and much lower than that in solution electrolytes (propylene carbonate (PC)): 1.6×10^{-10} m^2 s^{-1} [13,20]. Thus, better performance can be obtained by decreasing the thickness of the cathode and/or anode, although thin electrodes give low energy density too.

5. Conclusion

The electrochemical properties of the seven solvent-free polymer electrolytes were investigated and the charge–discharge performance of cells composed of the polymer electrolytes were compared. It was found the rate capability depends on the degree of cross-linking and the utilization of active material (cell capacity) depends on the precursor size. The polymer electrolytes including borate in the structure improved the high rate capability due to the high ionic conductivity and cation transference numbers. The homologue having smaller precursor size had fading capacity during the charge–discharge cycles. We have demonstrated good performance of charge–discharge cycles of 10 Wh class lithium battery made of all solid components which shows the potential for practical metal lithium batteries based on solvent-free polymer electrolytes.

Acknowledgements

The present study was supported by the NEDO project. The authors acknowledge Professor T. Fujinami for helpful discussion and also express their gratitude to Dr. K. Hayamizu and Professor W.S. Price for fruitful discussion.

References

[1] J. Kuratomi, T. Iguchi, T. Bando, Y. Aihara, T. Ono, K. Kuwana, J. Power Sources 97–98 (2001) 801.
[2] Y. Aihara, K. Hayamizu, K. Sugimoto, T. Bando, T. Iguchi, J. Kuratomi, T. Ono, K. Kuwana, J. Power Sources 97–98 (2001) 628.

[3] M. Watanabe, A. Nishimoto, Solid State Ion. 79 (1995) 306.
[4] M. Kono, E. Hayashi, M. Watanabe, J. Electrochem. Soc. 145 (1998) 1521.
[5] A. Killis, J.F. LeNest, A. Gandini, H. Cheradame, J. Polym. Sci., Polym. Phys. Ed. 19 (1981) 1073.
[6] D.W. Xia, J. Smid, J. Polym. Sci., Polym. Lett. 22 (1984) 617.
[7] M.A. Metha, T. Fujinami, Chem. Lett. 9 (1997) 915.
[8] M.A. Metha, T. Fujinami, T. Inoue, J. Power Sources 81–82 (1999) 724.
[9] Y. Kato, H. Ikuta, Y. Uchimoto, M. Wakihara, S. Yokoyama, Electrochem. Commun. 3 (2001) 128–130.
[10] K. Hayamizu, Y. Aihara, W.S. Price, J. Chem. Phys. 113 (2000) 4785.
[11] K. Hayamizu, Y. Aihara, W.S. Price, Electrochim. Acta 46 (2001) 1475.
[12] Y. Aihara, K. Hayamizu, K. Sugimoto, T. Bando, T. Iguchi, J. Kuratomi, T. Ono, K. Kuwana, J. Power Sources 97–98 (2001) 628.
[13] K. Hayamizu, K. Sugimoto, E. Akiba, Y. Aihara, T. Bando, W.S. Price, J. Phys. Chem. B 106 (2002) 547.
[14] M. Watanabe, M. Rikukawa, K. Sanui, N. Ogata, H. Kato, T. Kobayashi, Z. Ohtaki, Macromolecules 17 (1984) 2902.
[15] J. Evance, C.A. Vincent, P.G. Bruce, Polymer 28 (1987) 2324.
[16] T. Ohzuku, A. Ueda, J. Electrochem. Soc. 141 (1994) 2972.
[17] C. Menachen, E. Peled, L. Burstein, Y. Rosenberg, J. Power Sources 68 (1997) 277.
[18] J. Yamaki, M. Arakawa, S. Tobishima, T. Hirai, Proceedings of the Symposium on Lithium Batteries, vol. PV 87-1, The Electrochemical Society, New Jersey, 1987, 266 pp.
[19] K. Hayashi, Y. Nemoto, S. Tobishima, J. Yamaki, Electrochim. Acta 44 (1999) 2337.
[20] K. Hayamizu, Y. Aihara, S. Arai, C. Garcia-Martinez, J. Phys. Chem. B 103 (1999) 519.